SUPPORTING INFORMATION

Correlative analysis of Ni(II) coordination states in molten salts using a combination of X-ray and optical spectroscopies and simulations

Yang Liu,[a] Mehmet Topsakal,[b] Kaifeng Zheng,[a] Luis E. Betancourt,[b] Michael Woods,[c] Santanu Roy,[f] Nirmalendu Patra,[b] Denis Leshchev,[d] Phillip Halstenberg,[e] Dmitry S. Maltsev,[e,f] Sheng Dai,[e,f] Alexander S. Ivanov,[f] Vyacheslav S. Bryantsev,[f] James F. Wishart,[g] Ruchi Gakhar,[c]* Anatoly I. Frenkel,[a,g]* Simerjeet K Gill[b]**

[a] Department of Materials Science and Chemical Engineering, Stony Brook University, Stony Brook, NY 11794, USA

[b] Nuclear Science and Technology Department, Brookhaven National Laboratory, Upton, NY 11973, USA

[c] Advanced Technology of Molten Salts Department, Idaho National Laboratory, Idaho Falls, ID 83415, USA

[d] National Synchrotron Light Source II (NSLS-II), Brookhaven National Laboratory, Upton, New York 11973, United States

[e] Department of Chemistry, University of Tennessee, Knoxville, Tennessee 37996, USA

[f] Chemical Sciences Division, Oak Ridge National Laboratory, Oak Ridge, Tennessee 37831, United States

[g] Chemistry Division, Brookhaven National Laboratory, Upton, NY 11973, USA

Corresponding Authors

S.G.: Email: gills@bnl.gov, A.I.F.: Email: frenkel@bnl.gov, R.G: Email: ruchi.gakhar@inl.gov, J.F.W.: Email: wishart@bnl.gov

$NiCl_2$ solubility measurements in the studied salt mixtures:

The solubilities of $NiCl_2$ in the molten salt mixtures (LiCl-KCl, NaCl-$MgCl_2$, and LiCl-$ZnCl_2$) from 400–600 °C were measured using the isothermal saturation method reported in our previous study on molten salts.[1] Anhydrous $NiCl_2$, $ZnCl_2$, LiCl, KCl, and NaCl (99.99% purity) were purchased from Aldrich-APL. Anhydrous $MgCl_2$ (>98% purity, Sigma-Aldrich) was further purified by fractional distillation as described previously.[2] The salt mixtures for the solubility measurements were prepared in the glovebox. Nickel chloride was added in the amount exceeding its theoretical solubility limit in the corresponding salts at the respective temperatures. The resulting mixtures were fused at 400 °C (500 °C for NaCl-$MgCl_2$) under vacuum in quartz cells, which were then refilled with ultra-high purity nitrogen to maintain an inert atmosphere. The melts were periodically stirred for 6 h and then allowed to settle for an additional 24 h keeping the temperature constant. The precipitation of undissolved nickel chloride was visually verified during the experiments. Aliquots (two samples for each temperature) were collected from the upper clear part of the melt. After sampling the temperature was increased by 50 °C and the procedure was repeated: the melt was periodically stirred for several hours, then allowed to settle for at least 24 h and another two samples were collected from the upper clear part of the melt. After cooling down to room temperature, the salt samples were dissolved in a 3 wt% nitric acid solution and the nickel concentration was measured analytically by ICP-OES (inductively coupled plasma - optical emission spectrometry). A schematic diagram of the experimental apparatus used for the solubility measurements is shown in Figure S1, and the measured solubilities are presented in Table S1 and Figure S2.

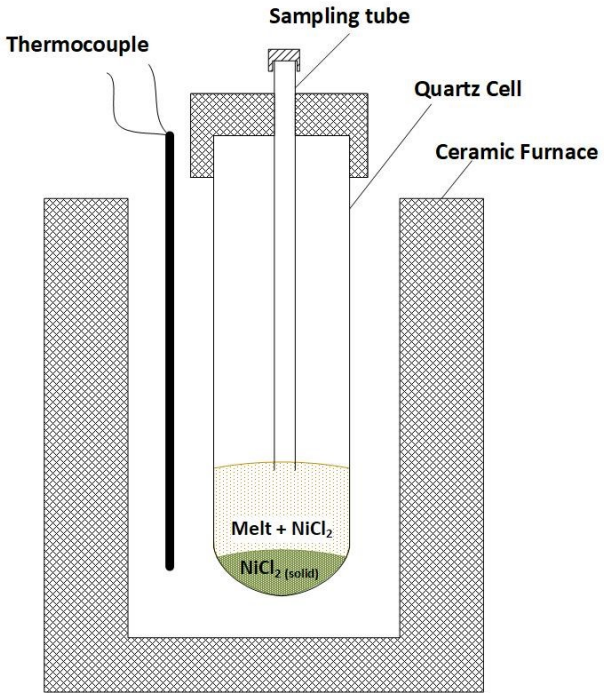

Figure S1. Diagram of the experimental apparatus for the $NiCl_2$ solubility measurements.

Table S1. Solubilities of $NiCl_2$ in three molten salt mixtures from 400–644 °C, in weight %. The

Temperature °C	LiCl-KCl	NaCl-$MgCl_2$	LiCl-$ZnCl_2$	Temperature °C	$ZnCl_2$
400	7.37	—	0.17	408	0.29
450	11.87	—	0.41	515	1.15
500	21.76	5.87	—	597	2.95
550	37.24	9.43	0.54	644	4.73
600	46.22	10.0	0.73	—	—

data for $ZnCl_2$ is from Kerridge and Sturton and converted from mole percent.[3]

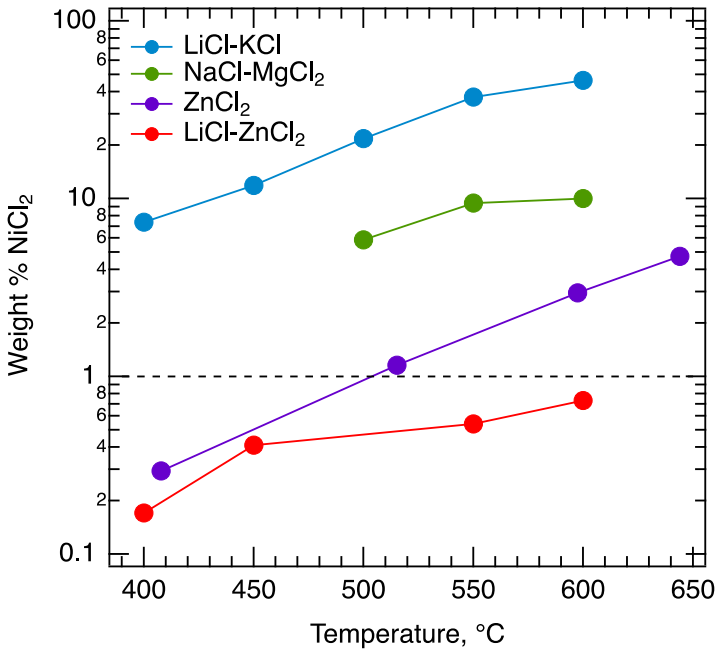

Figure S2. Solubilities of $NiCl_2$ (as weight %) in LiCl-KCl, NaCl-$MgCl_2$, $ZnCl_2$, and LiCl-$ZnCl_2$ from 400–644 °C. The 1 wt% loading of $NiCl_2$ used in the XAFS measurements is shown by the horizontal dotted line. The data for $ZnCl_2$ is from Kerridge and Sturton.[3]

Optical spectroscopy:

All spectroscopy experiments were performed in an argon glove box maintained at less than 1 ppm each O_2 and H_2O. The wavelength scale of the spectrophotometer (Agilent Cary 5000) over the range of 280 to 880 nm was verified and calibrated using a NIST-certified reference material consisting of an aqueous solution of didymium perchlorate permanently sealed in a high-quality far ultraviolet quartz cell, certificate number 72641. The cuvettes were baked in a vacuum oven at 120 °C overnight prior to loading the salt mixture and recording spectra.

MCR-ALS analysis:

The absorption coefficients for $NiCl_2$ in LiCl-KCl and NaCl-$MgCl_2$ are selected in the energy range from 8320.02 to 8498.09 eV. The PCA results are shown in Fig. 2c of the main text. The initial estimation of the C concentration profile and S resolved pure species profile are prepared

via the purest variable detection method. Two constraints are included in the MCR-ALS analysis: the non-negative value for C, S and the sum of weighting factors of all pure spectra at each reaction temperature step must be equal to 1. During the iteration process, the number of iterations were set to 50 and the convergence criterion was set as 0.1.

As shown in Figure 2 of the main text, our PCA analysis led us to select three components for the LiCl-KCl system and two components for the NaCl-$MgCl_2$ system to perform MCR-ALS analysis. We further validated the adequacy of using two components for both systems by comparing the results of two- and three-component MCR-ALS analyses. As illustrated in Figures S3 and S4, the inclusion of a third component does not provide additional information for the NaCl-$MgCl_2$ system. In contrast, the LiCl-KCl system benefits from three components, each containing distinguishable information.

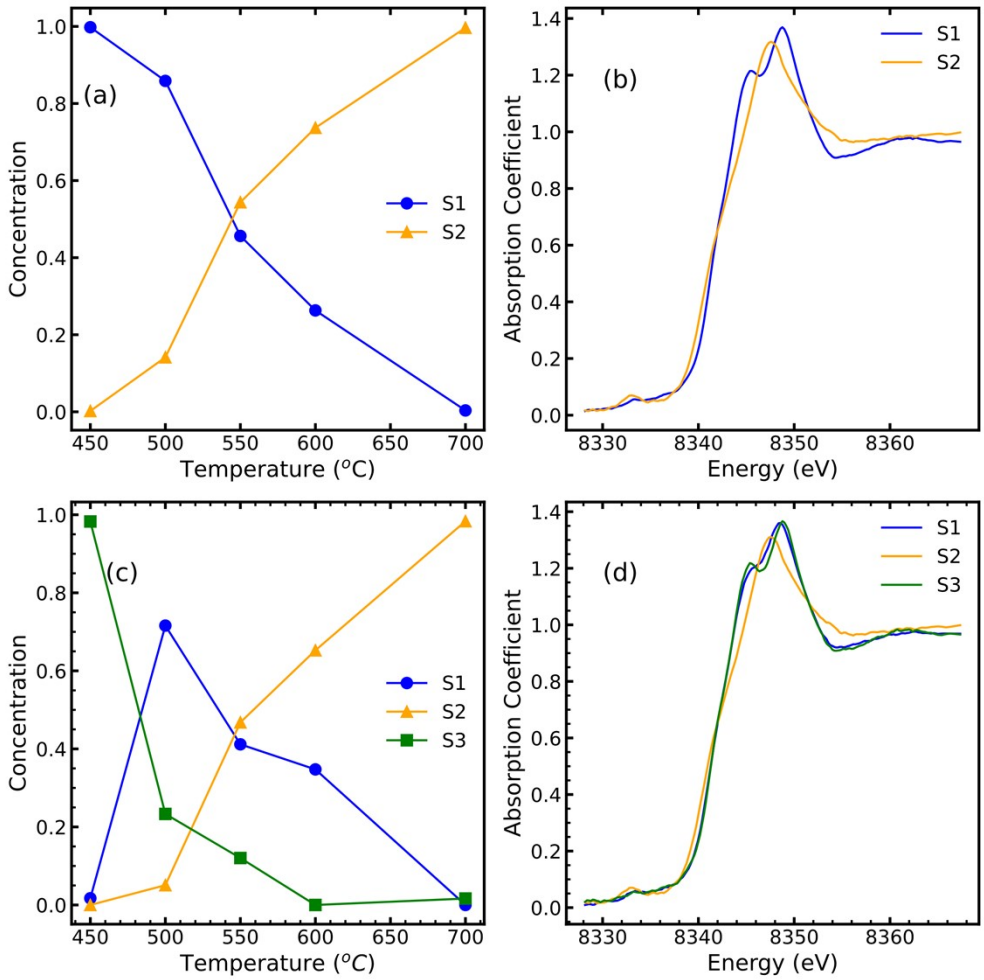

Figure S3. Comparison of two- or three-component MCR-ALS analysis of XANES spectra for the NaCl-$MgCl_2$ system

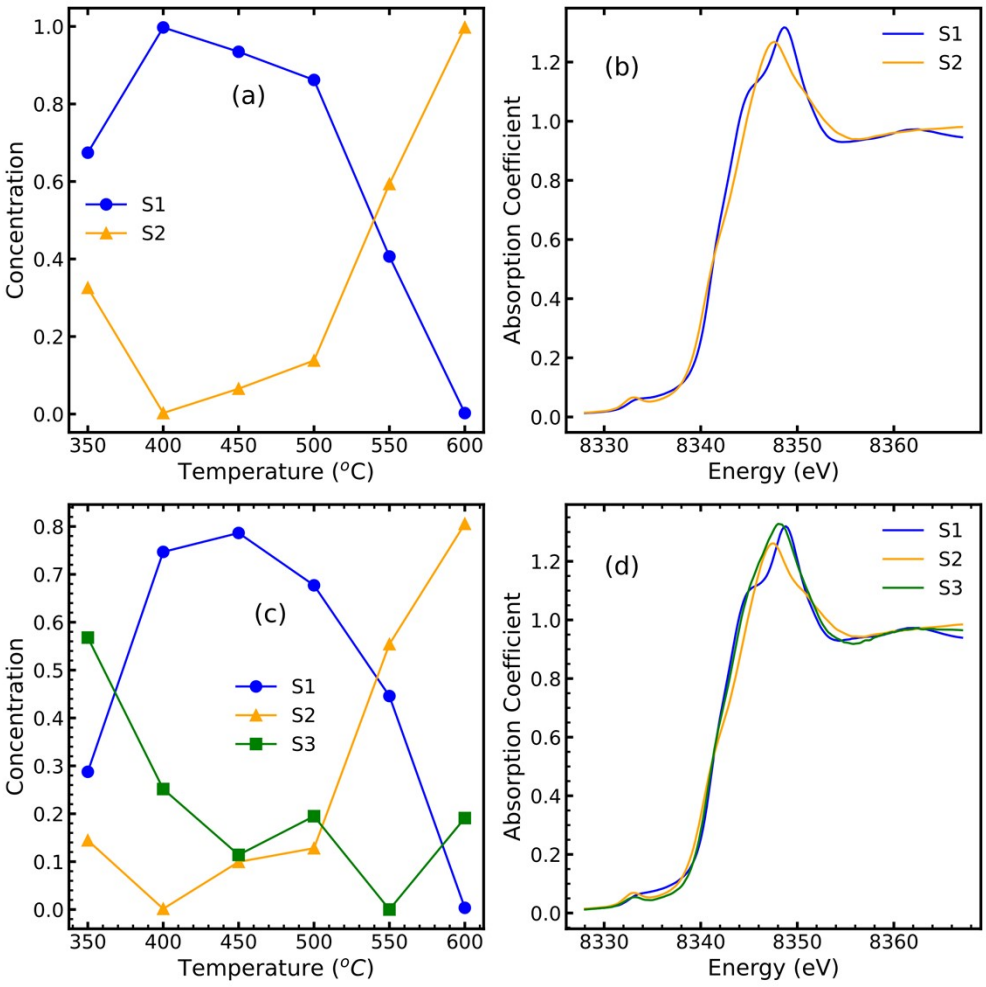

Figure S4. Comparison of two- or three-component MCR-ALS analysis of XANES spectra for the LiCl-KCl system

EXAFS spectroscopy:

The in-situ XAS experiment of the Ni K-edge was conducted at the Inner-Shell Spectroscopy beamline (ISS, 8-ID), at the National Synchrotron Light Source II (NSLS-II) of Brookhaven National Laboratory (BNL). The ISS beamline utilizes a damping wiggler source that provides a high flux (~5×10^{13} ph s^{-1}) and has an energy range from 4.9 keV to 36 keV, with a 0.5 mm × 0.5 mm (h × v) spot size. A custom-designed and built furnace was mounted at the beamline and used

to heat the samples in quartz capillaries from 20 to 600 °C. The Ni K-edge absorption spectra were acquired by tuning a cryogenically-cooled double crystal Si(111) monochromator, which enabled the energy fly-scanning mode. XAS spectra of the salts were recorded in the fluorescence mode with a passivated implanted planar silicon (PIPS) detector. Scanning and data acquisition times were ~1 minute per spectrum. More than 10 spectra were collected at each temperature step and averaged to further enhance the data quality. The absorption spectra of Ni foil standard samples were collected in both transmission and fluorescence modes.

Ab initio molecular dynamics (AIMD) and EXAFS modeling:

Based on our previous studies of Ni(II) speciation in pure $ZnCl_2$ and its mixture melts with KCl,[4,5] we first obtained initial configurations for the AIMD simulations at 600 °C through force fields-based MD simulations (1 femtosecond (fs) timestep) utilizing a polarizable ion model (PIM)[2,6-8] and the FIST module of the CP2K software.[9] For a system with 58 mol% LiCl, 42 mol% KCl, and 2 mol% $NiCl_2$, we performed the PIM runs replacing Ni with Mg as a proxy (as PIM parameters for Ni are unavailable)—1 nanosecond (ns) NPT (constant number of ions, pressure, and temperature) followed by 1 ns NVT (constant number of ions, volume, and temperature) runs at the experimental density of 1.592 g/cm^3. In the final NVT configuration, Mg was replaced with Ni to provide the initial structure for the AIMD simulations. Following the same approach, the initial structures for the AIMD simulations of a system comprising 22 LiCl, 78 $ZnCl_2$, and 2 $NiCl_2$ at density of 2.299 g/cm^3 and a system comprising 56 NaCl, 42 $MgCl_2$, and 2 $NiCl_2$ at density of 1.717 g/cm^3 were generated.

We performed the AIMD simulations of all three systems using a timestep of 1.0 fs and the Quickstep module of the CP2K 6.1 package.[10] We utilized the PBE exchange-correlation functional[11-14] with Grimme's D3 dispersion correction[15] and the MOLOPT(DZVP) basis set[16] in

conjunction with Goedecker-Teter-Hutter (GTH) pseudopotentials[17] for all ions. A 600 Ry cutoff for the plane wave basis was applied. A Nosé-Hoover chain thermostat[18,19] with a time constant of 1.0 picoseconds (ps) was used for the temperature coupling. Trajectories of at least 150 ps in length at 600 °C were generated for all three systems. For each trajectory, we discarded first 30 ps and used the remaining part for calculating EXAFS spectra and free energy profiles. We emphasize here that spin-unrestricted calculations considering different initial magnetizations should be performed before the MD steps to make sure that each system is in its ground electronic state with the expected spin moment. The orbital transformation method was employed with a FULL_ALL preconditioner and a conjugate gradient minimizer to achieve and accelerate the SCF convergence. For EXAFS calculations, we followed the same approach as discussed in our previous studies.[4,5]

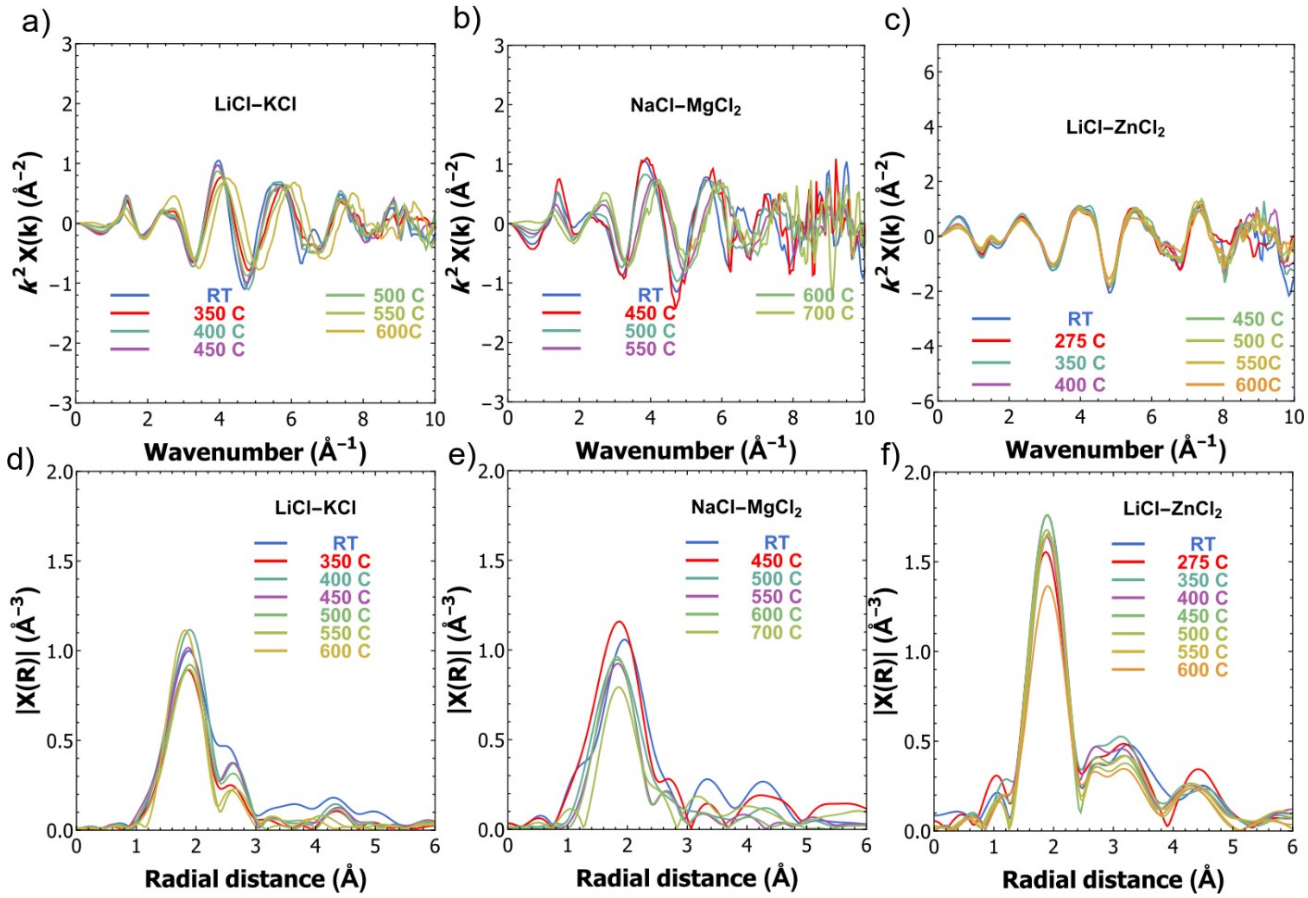

Figure S5. EXAFS spectra in a-c) *k*-space, d-f) *r*-space for $NiCl_2$ in LiCl-KCl, NaCl-$MgCl_2$ and LiCl-$ZnCl_2$.

References:

1. Liu, X. Y.; Ronne, A.; Yu, L. C.; Liu, Y.; Ge, M. Y.; Lin, C. H.; Layne, B.; Halstenberg, P.; Maltsev, D. S.; Ivanov, A. S.; Antonelli, S.; Dai, S.; Lee, W. K.; Mahurin, S. M.; Frenkel, A. I.; Wishart, J. F.; Xiao, X. H.; Chen-Wiegart, Y. Formation of three-dimensional bicontinuous structures via molten salt dealloying studied in real-time by in situ synchrotron X-ray nano-tomography. *Nat. Commun.* **2021,** *12*, 3441.
2. Wu, F.; Roy, S.; Ivanov, A. S.; Gill, S. K.; Topsakal, M.; Dooryhee, E.; Abeykoon, M.; Kwon, G.; Gallington, L. C.; Halstenberg, P.; Layne, B.; Ishii, Y.; Mahurin, S. M.; Dai, S.; Bryantsev, V. S.; Margulis, C. J. Elucidating Ionic Correlations Beyond Simple Charge Alternation in Molten $MgCl_2$–KCl Mixtures. *The Journal of Physical Chemistry Letters* **2019,** *10*, 7603-7610.
3. Kerridge, D. H.; Sturton, I. A. Fused zinc chloride part II: some solubility measurements. *Inorganica Chimica Acta* **1974,** *8*, 27-30.
4. Gill, S. K.; Huang, J.; Mausz, J.; Gakhar, R.; Roy, S.; Vila, F.; Topsakal, M.; Phillips, W. C.; Layne, B.; Mahurin, S.; Halstenberg, P.; Dai, S.; Wishart, J. F.; Bryantsev, V. S.; Frenkel, A. I. Connections between the Speciation and Solubility of Ni(II) and Co(II) in Molten $ZnCl_2$. *The Journal of Physical Chemistry B* **2020,** *124*, 1253-1258.
5. Roy, S.; Liu, Y.; Topsakal, M.; Dias, E.; Gakhar, R.; Phillips, W. C.; Wishart, J. F.; Leshchev, D.; Halstenberg, P.; Dai, S.; Gill, S. K.; Frenkel, A. I.; Bryantsev, V. S. A Holistic Approach for Elucidating Local Structure, Dynamics, and Speciation in Molten Salts with High Structural Disorder. *Journal of the American Chemical Society* **2021,** *143*, 15298-15308.
6. Ribeiro, M. C. C.; Wilson, M.; Madden, P. A. The nature of the "vibrational modes" of the network-forming liquid ZnCl2. *The Journal of Chemical Physics* **1998,** *109*, 9859-9869.
7. Ohtori, N.; Salanne, M.; Madden, P. A. Calculations of the thermal conductivities of ionic materials by simulation with polarizable interaction potentials. *The Journal of Chemical Physics* **2009,** *130*, 104507.
8. Ishii, Y.; Kasai, S.; Salanne, M.; Ohtori, N. Transport coefficients and the Stokes–Einstein relation in molten alkali halides with polarisable ion model. *Molecular Physics* **2015,** *113*, 2442-2450.
9. Hutter, J.; Iannuzzi, M.; Schiffmann, F.; VandeVondele, J. cp2k: atomistic simulations of condensed matter systems. *WIREs Computational Molecular Science* **2014,** *4*, 15-25.
10. VandeVondele, J.; Krack, M.; Mohamed, F.; Parrinello, M.; Chassaing, T.; Hutter, J. Quickstep: Fast and accurate density functional calculations using a mixed Gaussian and plane waves approach. *Computer Physics Communications* **2005,** *167*, 103-128.
11. Perdew, J. P.; Burke, K.; Ernzerhof, M. Generalized Gradient Approximation Made Simple. *Physical Review Letters* **1996,** *77*, 3865-3868.

12. Perdew, J. P.; Burke, K.; Ernzerhof, M. Perdew, Burke, and Ernzerhof Reply. *Physical Review Letters* **1998,** *80*, 891-891.

13. Zhang, Y.; Yang, W. Comment on ``Generalized Gradient Approximation Made Simple". *Physical Review Letters* **1998,** *80*, 890-890.

14. Perdew, J. P.; Ruzsinszky, A.; Csonka, G. I.; Vydrov, O. A.; Scuseria, G. E.; Constantin, L. A.; Zhou, X.; Burke, K. Restoring the Density-Gradient Expansion for Exchange in Solids and Surfaces. *Physical Review Letters* **2008,** *100*, 136406.

15. Grimme, S.; Antony, J.; Ehrlich, S.; Krieg, H. A consistent and accurate ab initio parametrization of density functional dispersion correction (DFT-D) for the 94 elements H-Pu. *Journal of Chemical Physics* **2010,** *132*.

16. VandeVondele, J.; Hutter, J. Gaussian basis sets for accurate calculations on molecular systems in gas and condensed phases. *Journal of Chemical Physics* **2007,** *127*.

17. Goedecker, S.; Teter, M.; Hutter, J. Separable dual-space Gaussian pseudopotentials. *Physical Review B* **1996,** *54*, 1703-1710.

18. Nosé, S. A unified formulation of the constant temperature molecular dynamics methods. *The Journal of Chemical Physics* **1984,** *81*, 511-519.

19. Martyna, G. J.; Klein, M. L.; Tuckerman, M. Nosé–Hoover chains: The canonical ensemble via continuous dynamics. *The Journal of Chemical Physics* **1992,** *97*, 2635-2643.